

Optical Properties of β'' -(ET)₂SF₅RSO₃ (R = CH₂CF₂, CHF₂CF₂): Changing Physical Properties by Chemical Tuning of the Counterion

I. Olejniczak,[†] B. R. Jones, Z. Zhu, J. Dong, and J. L. Musfeldt*

Department of Chemistry, State University of New York at Binghamton
Binghamton, New York 13902-6016

J. A. Schlueter, E. Morales, and U. Geiser

Chemistry and Materials Science Divisions, Argonne National Laboratory
9700 South Cass Avenue, Argonne, Illinois 60439

P. G. Nixon, R. W. Winter, and G. L. Gard

Department of Chemistry, Portland State University, Portland, Oregon 97207

Received April 26, 1999. Revised Manuscript Received September 22, 1999

We report the polarized infrared reflectance of β'' -(ET)₂SF₅CHFCF₂SO₃ as a function of temperature. This salt is a derivative of the first fully organic superconductor, β'' -(ET)₂SF₅-CH₂CF₂SO₃, where the nature of the alkyl group has been modified to contain a chiral center. This small chemical modification has a dramatic effect on the spectral and charge transport properties. The β'' -(ET)₂SF₅CHFCF₂SO₃ complex displays highly anisotropic behavior compared with the superconducting material; the essential difference is observed in the $\perp b$ direction where the interdimer interaction is weak, in agreement with recent theoretical calculations. The temperature dependence of key anion vibrational modes is discussed in terms of intermolecular hydrogen bonding within the anion pocket. That small chemical modifications of the anion template result in such striking changes in the physical properties suggests that the β'' -(ET)₂SF₅RSO₃ system is quite close to a Mott phase boundary.

I. Introduction

Bis(ethylenedithio)-tetrathiafulvalene, abbreviated as ET, is an electron-donor molecule which forms salts with various types of counterions. These complexes have received remarkable attention because superconductivity and other competing broken symmetry ground states are found in these materials.^{1–3} The highest superconducting transition temperatures to date are obtained with polymeric counterions in κ -(ET)₂Cu[N(CN)₂]Br (T_c = 11.6 K)⁴ and κ -(ET)₂Cu[N(CN)₂]Cl (T_c = 12.8 K at 0.3 kbar).⁵ One of the recent most fruitful strategies of new materials development involves incorporating large, discrete, chemically tunable anions into the complex,⁶ which allows the exploration of intermolecular interac-

tion effects on the physical properties. The κ -(ET)₂M-(CF₃)₄(1,1,2-trihaloethane) (M = Cu, Ag, Au; halogen = Cl, Br)⁷ and β'' -(ET)₂SF₅CH₂CF₂SO₃⁸ containing superconductors are examples of this effort. Here, the electronegative fluorine and/or oxygen end-groups on the counterions were chosen to interact with the ethylene groups on the ET building block molecule. In the β'' -(ET)₂SF₅RSO₃ system, small chemical modifications of the anion template can result in the stabilization of a spin–Peierls, semiconducting, metallic, or superconducting ground state.⁹ Possible changes to the template include: interchanging H and F atoms, lengthening or shortening the R group, replacing –SO₃ with –SeO₃, and replacing –SF₅ with –CF₃. It is β'' -(ET)₂SF₅-CHFCF₂SO₃, and a comparison with the β'' -(ET)₂SF₅-CH₂CF₂SO₃ superconductor, which is of interest here.

[†] Permanent address: Institute of Molecular Physics, Polish Academy of Sciences, Smoluchowskiego 17, Poznan, Poland.

(1) Ishiguro, T.; Yamaji, K.; Saito, G. *Organic Superconductors*, 2nd ed.; Springer-Verlag: Berlin, 1997.

(2) Wosnitzer, J. *Fermi Surfaces of Low Dimensional Organic Metals and Superconductors*; Springer-Verlag: Berlin, 1996.

(3) Williams, J. M.; Ferraro, J. R.; Carlson, K. D.; Geiser, U.; Wang, H. H.; Kini, A. M.; Whangbo, M. H. *Organic Superconductors*; Prentice-Hall: Englewood Cliffs, NJ, 1992.

(4) Kini, A. M.; Geiser, U.; Wang, H. H.; Carlson, K. D.; Williams, J. M.; Kwok, W.; Vandervoort, K. G.; Thompson, J. E.; Stupka, D. L.; Jung, D.; Whangbo, M. H. *Inorg. Chem.* **1990**, *29*, 2555.

(5) Williams, J. M.; Kini, A. M.; Wang, H. H.; Carlson, K. D.; Geiser, U.; Montgomery, L. K.; Pyrk, G. J.; Watkins, D. M.; Kommers, J. M.; Boryschuk, S. J.; Strieby Crouch, A. V.; Kwok, W. K.; Schirber, J. E.; Overmyer, D. L.; Jung, D.; Whangbo, M. H. *Inorg. Chem.* **1990**, *29*, 3262.

(6) Schlueter, J. A.; Williams, J. M.; Geiser, U.; Dudek, J. D.; Kelly, M. E.; Sirchio, S. A.; Carlson, K. D.; Naumann, D.; Roy, T.; Campana, C. F. *Adv. Mater.* **1995**, *7*, 634.

(7) Schlueter, J. A.; Carlson, K. D.; Geiser, U.; Wang, H. H.; Williams, J. M.; Kwok, W.-K.; Fendrich, J. A.; Welp, U.; Keane, P. M.; Dudek, J. D.; Komosa, A. S.; Naumann, D.; Roy, T.; Schirber, J. E.; Bayless, W. R.; Dadrill, B. *Physica C* **1994**, *233*, 379.

(8) Geiser, U.; Schlueter, J. A.; Wang, H. H.; Kini, A. M.; Williams, J. M.; Sche, P. P.; Zakowicz, J. I.; VanZile, M. L.; Dudek, J. D. *J. Am. Chem. Soc.* **1996**, *118*, 9996.

(9) Ward, B. H.; Schlueter, J. A.; Geiser, U.; Wang, H. H.; Morales, E.; Parakka, J.; Thomas, S. Y.; Williams, J. M.; Nixon, P. G.; Winter, R. W.; Gard, G. L.; Koo, H. J.; Whangbo, M. H. *Chem. Mater.*, submitted for publication.

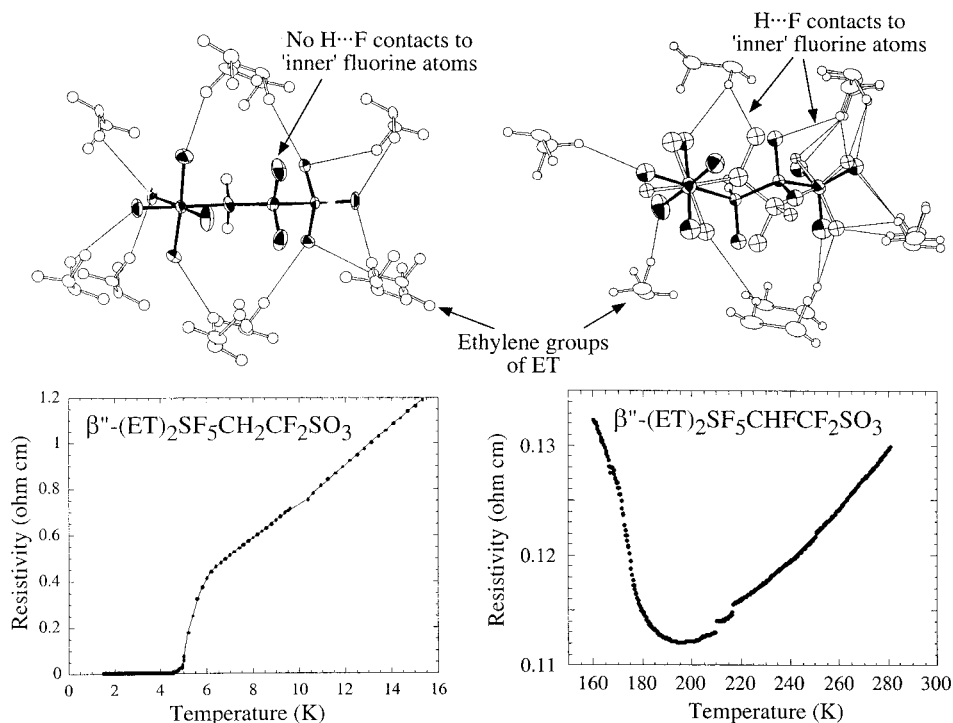


Figure 1. Structure of the anion pocket in $\beta''\text{-(ET)}_2\text{SF}_5\text{CH}_2\text{CF}_2\text{SO}_3$ and $\beta''\text{-(ET)}_2\text{SF}_5\text{CHFCF}_2\text{SO}_3$ at 300 K. The insets display the temperature-dependent resistivity for each of the aforementioned compounds.

The crystal structure of $\beta''\text{-(ET)}_2\text{SF}_5\text{CHFCF}_2\text{SO}_3$ displays the low-dimensional architecture which is typical of many β -type molecular conductors, with two-dimensional conducting planes separated by a charge storage layer.¹⁰ Stacks of ET dimers are observed along a ; the ethylene groups of ET molecules are disordered at room temperature and become ordered below 200 K. In the conducting plane, the best intermolecular contacts are along the b direction; these are facilitated by S...S interactions. The unit cell parameters for $\beta''\text{-(ET)}_2\text{SF}_5\text{CHFCF}_2\text{SO}_3$ are almost identical to those of the superconductor. The main difference between the two compounds is counterion ordering. The anion in the superconductor is ordered whereas in the $\beta''\text{-(ET)}_2\text{SF}_5\text{CHFCF}_2\text{SO}_3$ salt it is disordered at room temperature, locking into two conformations at low temperature. The other difference concerns hydrogen bonding. It is interesting that no short contacts from $-\text{CH}_2\text{CF}_2-$ fluorine atoms are observed with hydrogen atoms of ET in the superconductor, as shown in Figure 1. However, in $\beta''\text{-(ET)}_2\text{SF}_5\text{CHFCF}_2\text{SO}_3$, there are important short contacts between the fluorines on the $-\text{CHFCF}_2-$ part of the anion and ET's hydrogen atoms, likely giving rise to the anion disorder. Here, the sulfonate oxygen atoms as well as both the interior and peripheral fluorine atoms compete for intermolecular contacts with the hydrogen atoms of the ethylene units on the ET molecule. A "too many cooks in the kitchen" scenario causes disorder within the anion pocket and destroys the low-temperature metallic state, resulting in a metal \rightarrow insulator transition in the $\beta''\text{-(ET)}_2\text{SF}_5\text{CHFCF}_2\text{SO}_3$ system. This is in contrast to the situation in the superconductor, where the anions are ordered and only the $-\text{SF}_5$ and $-\text{SO}_3$ end groups are involved in intermolecular hydrogen bonding.⁸

While a number of physical property studies have focused on the $\beta''\text{-(ET)}_2\text{SF}_5\text{CH}_2\text{CF}_2\text{SO}_3$ superconductor

($T_c = 5.2$ K),^{12–17} much less is known about the $\beta''\text{-(ET)}_2\text{SF}_5\text{CHFCF}_2\text{SO}_3$ system. The 300 K DC conductivity is $\approx 7.4 \Omega^{-1} \text{ cm}^{-1}$ in the ab plane.¹⁰ A metal \rightarrow insulator transition near 175 K has been reported; some hysteresis is observed in the transition range. The spin susceptibility determined by ESR is in line with the aforementioned temperature dependence of the resistivity.¹⁰ That χ tends toward zero below 175 K suggests that the spins are paired in a singlet state in the low-temperature phase. Band structure calculations predict that the Fermi surface of both the superconductor and the $\beta''\text{-(ET)}_2\text{SF}_5\text{CHFCF}_2\text{SO}_3$ derivative consists of a pair of one-dimensional bands and a two-dimensional hole pocket.^{10,11} In the superconductor, magnetoresistance measurements have found the hole pocket to be highly elliptical, covering $\approx 5\%$ of the first Brillouin zone.¹² On the basis of high- and low-temperature structural information, interaction energies for both systems were calculated using the extended Hückel tight-binding

(10) Schlueter, J. A.; Ward, B. H.; Geiser, U.; Wang, H. H.; Kini, A. M.; Parakka, J.; Morales, E.; Koo, H. J.; Whangbo, M. H.; Nixon, P. G.; Winter, R. W.; Gard, G. L. *J. Mater. Chem.*, submitted for publication.

(11) Koo, H.-J.; Whangbo, M.-H.; Dong, J.; Olejniczak, I.; Musfeldt, J. L.; Schlueter, J. A.; Geiser, U. *Solid State Commun.*, in press.

(12) Beckmann, D.; Wanka, S.; Wosnitza, J.; Schlueter, J. A.; Williams, J. M.; Nixon, P. G.; Winter, R. W.; Gard, G. L.; Ren, J.; Whangbo, M.-H. *Eur. Phys. J.* **1998**, *B1*, 295.

(13) Wanka, S.; Hagel, J.; Beckmann, D.; Wosnitza, J.; Schlueter, J. A.; Williams, J. M.; Nixon, P. G.; Winter, R. W.; Gard, G. L. *Phys. Rev. B* **1998**, *57*, 3084.

(14) Wosnitza, J.; Goll, G.; Beckmann, D.; Wanka, S.; Schlueter, J. A.; Williams, J. M.; Nixon, P. G.; Winter, R. W.; Gard, G. L. *Physica B* **1998**, *246–247*, 104.

(15) Wosnitza, J.; Wanka, S.; Qualls, J. S.; Brooks, J. S.; Mielke, C. H.; Harrison, N.; Schlueter, J. A.; Williams, J. M.; Nixon, P. G.; Winter, R. W.; Gard, G. L. *Synth. Met.*, in press.

(16) Su, X.; Zuo, F.; Schlueter, J. A.; Williams, J. M.; Nixon, P. G.; Winter, R. W.; Gard, G. L. *Phys. Rev. B* **1999**, *59*, 4376.

(17) Wosnitza, J.; Wanka, S.; Hagel, J.; Häußler, R.; Löhneysen, H. v.; Schlueter, J. A.; Geiser, U.; Nixon, P. G.; Winter, R. W.; Gard, G. L. *Phys. Rev. B*, submitted for publication.

method. It was found that while the interstack interactions are similar in both compounds, the interaction between dimers in the donor stack of the β'' -(ET)₂SF₅-CHFCF₂SO₃ complex is quite weak at low temperature, which is conducive to electron localization.^{10,11} In contrast, the interdimer interaction remains substantial in the superconductor.

To provide further information on the nature of the vibrational and electronic processes in this class of materials, we have investigated the polarized infrared response of β'' -(ET)₂SF₅CHFCF₂SO₃ as a function of temperature. We discuss our results in comparison with the newly discovered β'' -(ET)₂SF₅CH₂CF₂SO₃ superconductor,¹⁸ the β'' -(ET)₄[Fe(ox)₃H₃O]C₆H₅CN (ox = oxalate) compound, and other β -phase ET-based superconductors.^{19–21} Our overall goal is to understand the correlation between the chemical structure of the anion and the ground-state physical properties.

II. Experimental Section

High quality single crystals of β'' -(ET)₂SF₅RSO₃ ($1.2 \times 10 \times 0.3$ mm³) were grown via electrochemical techniques in an H-cell at Argonne National Laboratory.¹⁰ Both β'' -(ET)₂SF₅-CH₂CF₂SO₃ and β'' -(ET)₂SF₅CHFCF₂SO₃ samples have been studied in our laboratory. The crystals are elongated plates with shiny surfaces; the long axis of the crystal is the *b* axis and the large face containing the conducting *ab* plane.²²

Polarized middle and near-infrared reflectance measurements were performed with a Bruker Equinox 55 FTIR spectrometer (600–12000 cm⁻¹) in combination with a Bruker IR Scope II. Nitrogen-cooled detectors MCT and InSb and standard polarizers were used to cover the aforementioned energy range. Temperature control was achieved with an open-flow Oxford Microstat He cryostat system, which fit between the 15 \times objective and the sample stage. The temperature dependence of the middle and near-infrared spectra was measured on warming from 4 to 300 K, with special attention to the 175 K metal \rightarrow insulator transition regime. Care was taken to equilibrate the sample at each temperature.

The frequency range of the measurement allows us to make a Kramers–Kronig analysis to obtain the optical constants of the material. These include the frequency dependent conductivity, $\sigma_1(\omega)$, the dielectric constant, $\epsilon_1(\omega)$, and the effective mass $m^*(\omega)$.²³ The high-frequency extrapolation to the Kramers–Kronig phase shift integral was performed as $\omega^{-1.8}$, and the low-frequency extrapolation was made as a constant, appropriate for a semiconducting sample.²³ Small level differences often result from using a limited frequency range in a Kramers–Kronig analysis; that the $R = \text{CHFCF}_2$ spectrum along *b* is so similar to that of the superconductor (which was measured over a much broader range) is good indication of reliable Kramers–Kronig treatment.

III. Results

A. Room–Temperature Spectra. Figure 2 displays the 300 K reflectance of β'' -(ET)₂SF₅CHFCF₂SO₃ in the

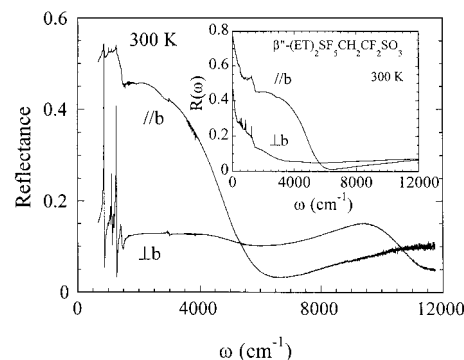


Figure 2. Polarized infrared reflectance of β'' -(ET)₂SF₅-CHFCF₂SO₃ at 300 K. The inset displays similar data on the β'' -(ET)₂SF₅CH₂CF₂SO₃ superconducting compound. Both $\parallel b$ and $\perp b$ polarizations are shown.

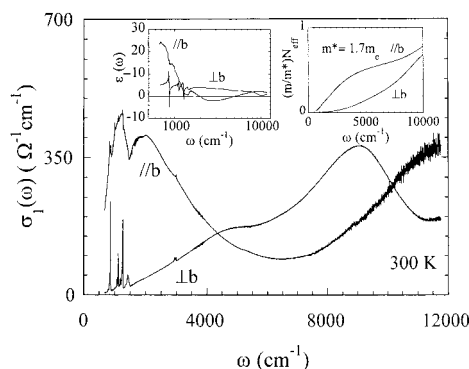


Figure 3. Room-temperature frequency dependent conductivity of β'' -(ET)₂SF₅CHFCF₂SO₃. Left inset: dielectric constant of β'' -(ET)₂SF₅CHFCF₂SO₃ as a function of frequency. Right inset: conductivity sum rule for β'' -(ET)₂SF₅CHFCF₂SO₃.

two principle polarization directions. The reflectance in the *b* direction (interstack) is significantly larger than that in the $\perp b$ direction ($\sim \parallel a$, i.e., ET stack) and shows a well-defined drop in the middle-infrared region. In this direction, a strong similarity in overall shape and reflectance level is observed with that of the superconducting sample (inset, Figure 2). In the $\perp b$ polarization, the reflectance is low and flat in the middle-infrared, in contrast to the overdamped and more two-dimensional behavior of β'' -(ET)₂SF₅CH₂CF₂SO₃.¹⁸ As in the superconductor, most of the vibrational structure is observed perpendicular to *b*, where ET dimers are stacked in a face-to-face fashion and anion dipole moments are directed.

The 300 K frequency dependent conductivity of β'' -(ET)₂SF₅CHFCF₂SO₃ is shown in Figure 3. Optically, this material is highly anisotropic. In fact, the quasi-one-dimensionality is reminiscent of β'' -(ET)₄[Fe(ox)₃-H₃O]C₆H₅CN (ox = oxalate) superconductor ($T_c = 7$ K) rather than β'' -(ET)₂SF₅CH₂CF₂SO₃ or the other β -type superconductors ((ET)₂I₃, (ET)₂AuI₂).^{19,20} A broad electronic band centered near 2000 cm⁻¹ is found in the $\parallel b$ direction (Figure 3). This low-lying infrared excitation was also observed in both $\parallel b$ and $\perp b$ polarizations in β'' -(ET)₂SF₅CH₂CF₂SO₃, although it was much stronger along *b*.¹¹ It is notable that the responses of the superconductor and the R=CHFCF₂ derivative are almost identical in the highly conducting direction. On the basis of the overall low level of middle-infrared conductivity of the R=CHFCF₂ sample in the $\perp b$ direction, there is little interaction between dimers

(18) Dong, J.; Musfeldt, J. L.; Schlueter, J. A.; Williams, J. M.; Nixon, P. G.; Winter, R. W.; Gard, G. L. *Phys. Rev. B*, submitted for publication.

(19) Jacobsen, C. S.; Williams, J. M.; Wang, H. H. *Solid State Commun.* **1985**, *54*, 937.

(20) Jacobsen, C. S.; Tanner, T. B.; Williams, J. M.; Geiser, U.; Wang, H. H. *Phys. Rev. B* **1987**, *35*, 9605.

(21) Kurmoo, M.; Graham, A. W.; Day, P.; Coles, S. J.; Hursthouse, M. B.; Caulfield, J. L.; Singleton, J.; Pratt, F. L.; Hayes, W.; Ducasse, L.; Guionneau, P. *J. Am. Chem. Soc.* **1995**, *117*, 12209.

(22) In the superconductor, the high quality of the crystal samples was confirmed by the sharp superconducting transition at 5.2 K in the AC susceptibility.⁸

(23) Wooten, F. *Optical Properties of Solids*; Academic Press: New York, 1972.

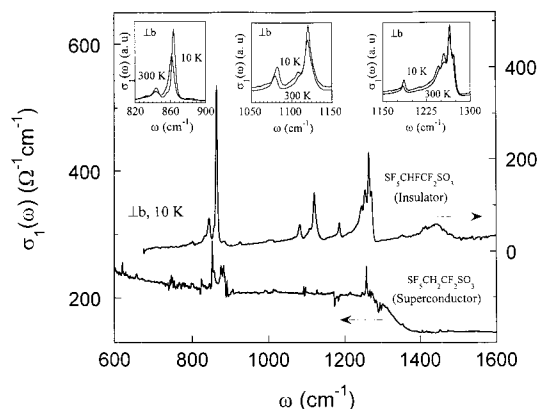


Figure 4. Detailed frequency dependent conductivity of β'' -(ET) $_2\text{SF}_5\text{CHFCF}_2\text{SO}_3$ and β'' -(ET) $_2\text{SF}_5\text{CH}_2\text{CF}_2\text{SO}_3$ at 10 and 300 K, along the $\perp b$ direction, in the SF_5 and SO_3 stretching vibrational region of the anion. Note that the curves are offset for clarity; separate y -axis scales are provided. Insets show close-up views of specific vibrational modes.

along the stacks, in agreement with recent theoretical calculations.¹⁰ However, the low-energy $\perp b$ electronic features of the derivative differ significantly from the superconductor; both the strong absorption near 9000 cm^{-1} and the shoulder near 4900 cm^{-1} are currently of unknown origin.

The left-hand inset of Figure 3 displays the 300 K frequency dependent dielectric constant of β'' -(ET) $_2\text{SF}_5\text{CHFCF}_2\text{SO}_3$. Here, $\epsilon_1(\omega)$ is positive for both polarizations at low frequency, extrapolating to static values of ≈ 30 and 5 for $\parallel b$ and $\perp b$, respectively. There is strong dielectric contrast at low frequencies, in agreement with results on the β'' -(ET) $_2\text{SF}_5\text{CH}_2\text{CF}_2\text{SO}_3$ superconductor. The high energy dielectric constant $\epsilon_1(\infty)$, is ≈ 2 for both polarizations. From the zero crossing of ϵ_1 for $\parallel b$, we estimate a screened plasma frequency of $\approx 4800 \text{ cm}^{-1}$, which is very close to the value of $\approx 4700 \text{ cm}^{-1}$ determined for the superconductor. The partial sum rule on the conductivity (right-hand inset of Figure 3) relates the oscillator strength to the effective mass and the effective number of carriers per formula unit participating in optical transitions. Assuming a carrier concentration resulting from 1 carrier per dimer, we find $m^*_b \approx 1.7m_e$. In the superconductor, $m^*_b \approx 2m_e$.

B. Temperature Dependence. In general, the spectral changes of β'' -(ET) $_2\text{SF}_5\text{CHFCF}_2\text{SO}_3$ with temperature through the metal \rightarrow insulator transition are fairly weak. That the spectral changes are small is natural, as the change in resistivity through the 175 K metal \rightarrow insulator transition is also modest. In the $\parallel b$ direction, the overall reflectance level is slightly higher in the low-temperature phase, but the spectrum is otherwise unchanged. We concentrate our discussion on the spectra in the ET stacking direction ($\perp b$).

Figure 4 shows a comparison of the $\perp b$ spectra of β'' -(ET) $_2\text{SF}_5\text{CHFCF}_2\text{SO}_3$ with that of the β'' -(ET) $_2\text{SF}_5\text{CH}_2\text{CF}_2\text{SO}_3$ superconductor, as well as close-up views of the detailed temperature dependence of several specific vibrational modes. In this direction, there are small frequency shifts in some of the vibrational modes and splitting is slightly more pronounced with decreasing temperature. As previously mentioned, the $\perp b$ spectrum displays a lower energy excitation appearing as a shoulder near 4700 cm^{-1} and a broad higher energy

band centered near 9000 cm^{-1} . The upper structure develops a very weak doublet structure at low temperature (not shown), indicative of additional localization in the semiconducting phase.

IV. Discussion

A. Electronic Excitations. One of the most striking features of the optical conductivity in β'' -(ET) $_2\text{SF}_5\text{CHFCF}_2\text{SO}_3$ is the overall character of the spectra, which is weakly conducting at room temperature with a low-lying electronic band in the middle-infrared at $\approx 2000 \text{ cm}^{-1}$ in the $\parallel b$ direction. As discussed previously, such infrared localization is observed in β'' -(ET) $_2\text{SF}_5\text{CH}_2\text{CF}_2\text{SO}_3$, several other β -type conductors and superconductors ((ET) $_2\text{I}_3$, (ET) $_2\text{AuI}_2$, and (ET) $_2\text{I}_2\text{Br}$),^{19,20} β'' -(ET) $_4[\text{Fe}(\text{ox})_3\text{H}_3\text{O}]\text{C}_6\text{H}_5\text{CN}$ (ox = oxalate),²¹ and α -(ET) $_2\text{I}_3$,²⁴ which is similar to the β -phase in structure. Within an electronic band structure picture, such a low-energy excitation is assigned as an interband transition, as in the case for the $\text{R} = \text{CH}_2\text{CF}_2$ superconductor.¹¹ In reality, organic solids are probably near $4t \approx U$ rather than in the one-electron limit (where the band structure is appropriate) or the large U limit (where localized models are fully appropriate). Here, t is the transfer integral, $4t$ is the bandwidth, and U is the on-site Coulomb repulsion. Our estimates of effective mass for the β'' -(ET) $_2\text{SF}_5\text{RSO}_3$ materials are in line with $4t \approx U$. Therefore, electronic correlations and low carrier densities may also be mechanisms which contribute to this localization phenomena.

Theoretical approaches based on the Hubbard and other localized models have helped us to understand the microscopic origin of the middle-infrared localization.^{25–30} On the basis of well-known structural considerations, the typical unit of consideration in these models is the dimer. In this picture, the ground state of an ET-based molecular conductor consists of one hole shared over two sites. Therefore, the main excited-state available to this molecular system is to have the charge localized on one molecule in the dimer. Thus, the energy of the middle-infrared electronic band provides an experimental measure of the on-site Coulomb repulsion, U .³¹ For metals in close proximity to the Mott metal–insulator transition, the theory predicts that the optical conductivity shows the development of a Drude peak, a resonance at an energy U due to the transitions between upper and lower Hubbard bands, and an enhancement of spectral weight at $U/2$ below a critical temperature.^{29,32} Thus, we can assign the low-lying middle-infrared band

(24) Železný, V.; Petzelt, J.; Swietlik, R.; Gorshunov, B. P.; Volkov, A. A.; Kozlov, G. V.; Schweitzer, D.; Keller, H. J. *J. Phys. Fr.* **1990**, *51*, 869.

(25) Tajima, H.; Yakushi, K.; Kuroda, H.; Saito, G. *Solid State Commun.* **1985**, *56*, 159.

(26) Ugawa, A.; Ojima, G.; Yakushi, K.; Kuroda, H. *Phys. Rev. B* **1988**, *38*, 5122.

(27) Yartsev, V. M.; Drozdova, O. O.; Semkin, V. N.; Vlasova, R. M. *J. Phys. I Fr.* **1996**, *6*, 1673.

(28) McKenzie, R. H. *Comments Condens. Mater. Phys.* **1998**, *18*, 309.

(29) Bulka, B. R. Proceedings of the 1998 Conference on Molecular Crystals, Gdansk, Poland. *Mol. Phys. Rep.*, in press.

(30) Fortunelli, A.; Painelli, A. *Phys. Rev. B* **1997**, *55*, 16088.

(31) In an optical spectrum, the energy of such an excitation is actually $U - V \approx U$ if V is small. Here, U is the on-site Coulomb repulsion and V is the near-neighbor repulsion.

(32) Rozenberg, M. J.; Kotliar, G.; Kajueter, H. *Phys. Rev. B* **1996**, *54*, 8452.

in the $\parallel b$ direction either to an interband transition (within a band structure picture) or to an effective U excitation due to electronic correlation effects. Effective masses for both the superconductor and β'' -(ET)₂SF₅CHFCF₂SO₃ derivative sample support moderate many-body effects in these systems, so a complete microscopic description of this excitation is an important theoretical challenge.

An assignment for the strong electronic absorptions which appears near 4700 and 9000 cm⁻¹ in the $\perp b$ spectrum of the derivative sample is currently elusive. That these excitations are absent in the superconductor¹⁸ and cannot be accounted for within electronic band structure calculations,^{11,33} suggests that they are likely either correlation- or disorder-related. Further investigation is in progress.

The possibility of Anderson localization due to random potentials connected with disorder in the anion pockets is another interesting issue. Unfortunately, this kind of effect cannot be separated from electron-electron interactions, as it leads to rather complex behavior which has proved to be difficult to describe.³⁴ Although evidence of such a localization was found from NMR studies of the organic superconductor β_L -(ET)₂I₃,³⁵ it is related to an incommensurate modulated structure and substantial disorder in the ET molecular sublattice. In both materials under study here, the ET molecules become ordered at low temperatures, suggesting that Anderson localization, if present, is less important than many-body effects.

B. Vibrational Features. The vibrational features of β'' -(ET)₂SF₅CHFCF₂SO₃ are well-resolved in the $\perp b$ polarization, but show weak temperature dependence overall (Figure 4). The modes resulting from electron-phonon coupling of donor vibrations with the lowest electronic band near 4900 cm⁻¹ are very weak because of the high frequency of this electronic excitation. Nevertheless, we assign features at 1184 cm⁻¹ and two multiplet structures centered at about 1260³⁶ and 1420 cm⁻¹ as related to out-of-plane CH bending (ν_{38} (b_{2g})), symmetric CH bending (ν_5 (a_g)) and C=C stretching ν_2 (a_g), respectively.³⁷⁻³⁹ The temperature dependence of these modes, which become sharper at low temperature, is due to enhancement and red-shifting of the lowest electronic band.

Because intermolecular hydrogen bonding is anticipated between the ethylene end groups of the ET molecule and the -SF₅ and -SO₃ end groups of the counterion, the vibrational features of anion, especially the modes associated with the -SF₅ and -SO₃ groups, may provide information about this interaction. On the basis of existing reference spectra for the -SO₃ and

-SF₅ functional groups,^{40,41} we assign the doublets between 1079 and 1120 and 844-862 cm⁻¹ (see insets in Figure 4) to the stretching vibrations of the -SO₃ and -SF₅ groups in the anion, respectively. In particular, these modes are very broad and strong, probably due to the significant hydrogen bonding formed between anion and the ethylene end unit of the ET molecules, their doublet structure being connected with the two possible conformations of anion in the crystal structure.⁴² The width of these features also suggests disorder in the intermolecular hydrogen bonding within the anion pockets. The doublets display the usual sharpening and a small blue shift of 1-3 cm⁻¹ with decreasing temperature. Overall, the vibrational features indicate only a weak structural change and probably some reduction of hydrogen bonding in the anion pocket with decreasing temperature. Thus, the metal \rightarrow insulator transition at 175 K is nearly invisible in our vibrational studies.

In general, a comparison of the $\perp b$ spectrum of β'' -(ET)₂SF₅CHFCF₂SO₃ and the superconductor reveals significant differences in vibrational features. The vibrational modes are very strong and broad in the derivative due to an insulator-type response. The counterion modes, discussed in the previous paragraph, are especially pronounced; however, the vibronic coupling is fairly weak overall. Compared to the derivative, the superconductor displays even less prominent vibronic modes and weaker anion modes as expected for the more metallic system. The significant buildup of oscillator strength with decreasing temperature in the far-infrared $\sigma_1(\omega)$ at low frequencies may be related to increased interdimer interaction in the superconductor;¹⁸ note that only the tail of this oscillator strength is seen in Figure 4. No such residual conductivity is observed in the spectrum of β'' -(ET)₂SF₅CHFCF₂SO₃.

Finally, there is currently some uncertainty regarding the nature of the low-temperature semiconducting ground state in β'' -(ET)₂SF₅CHFCF₂SO₃, with both density wave and antiferromagnetic ground states as two possible configurations. Both possibilities are consistent with the susceptibility data, which show that the spins are paired at low temperature. Results of recent theoretical calculations suggest that a charge density wave state may be favored.⁴³ However, our low-temperature infrared spectra do not display evidence of coupling to a charge modulation. Such vibronic coupling is typically very strong and not easily missed in a commensurate density wave system. Therefore, we find that the antiferromagnetic low-temperature ground state is more likely.

V. Conclusion

We report the polarized infrared reflectance of β'' -(ET)₂SF₅CHFCF₂SO₃ as a function of temperature. Here, disorder in the anion pocket results in a metal \rightarrow insulator transition at 175 K, the doublet structure in the vibrational pattern supporting a low-temperature

(33) Whangbo, M.-H. Unpublished results.

(34) Mott, N. F. *Metal-Insulator Transitions*, 2nd ed.; Taylor & Francis: London, 1990.

(35) Vainrub, A.; Vija, S.; Lippmaa, E.; Prigodin, V.; Beha, R.; Mehring, M. *Phys. Rev. Lett.* **1992**, *69*, 3116.

(36) The narrow band at 1264 cm⁻¹ superimposed on the vibronic structure at 1260 cm⁻¹ is probably due to stretching vibration of the CF bond of the anion—see upper right-hand panel in Figure 4.

(37) Eldridge, J. E.; Homes, C. C.; Williams, J. M.; Kini, A. N.; Wang, H. H.; *Spectrochimica Acta* **1995**, *51A*, 947.

(38) Eldridge, J. E.; Xie, Y.; Wang, H. H.; Williams, J. M.; Kini, A. M.; Schlueter, J. A. *Spectrochimica Acta* **1996**, *52A*, 45.

(39) Eldridge, J. E.; Xie, Y.; Lin, Y.; Homes, C.; Wang, H. H.; Williams, J. M.; Kini, A. M.; Schlueter, J. A. *Spectrochimica Acta* **1997**, *53A*, 565.

(40) Evans, J. C.; Bernstein, H. J. *Can. J. Chem.* **1955**, *33*, 1270.

(41) Eggers, D. F.; Wright, H. E.; Robinson, D. W. *J. Chem. Phys.* **1961**, *35*, 1045.

(42) It is unlikely that the doublet structure is related to dimerization as these are anion modes, and the splitting is fairly large.

(43) Whangbo, M.-H. Unpublished results.

"locking" into two configurations. Despite the aforementioned metal \rightarrow insulator transition, the spectra are characteristic of a highly one-dimensional material over the full temperature range, in agreement with theoretical results on the importance of localization in the derivative material. We compare the infrared spectra of the R=CHFCF₂ sample with that of the superconductor to ascertain differences in the intermolecular hydrogen bonding. That counterion tunability has such a strong effect on the physical properties of the β'' -(ET)₂SF₅RSO₃ system supports the supposition that the chemical environment is very important to the nature of electron-electron interactions. Electronic structure features in the β'' -(ET)₂SF₅RSO₃ system remain an area of further investigation.

Acknowledgment. Work at SUNY-Binghamton was supported by Grant No. DMR-9623221 from the Division of Materials Research at the National Science

Foundation and by the National Science Foundation/North Atlantic Treaty Organization under a Postdoctoral Fellowship in Science and Engineering for Visiting Scientists from Cooperation Partner Countries (DGE 9804462). We are also grateful for the equipment provided through the Division of Materials Research/Instrumentation for Materials Research at the National Science Foundation (DMR 9802788). Work at Argonne National Laboratory was supported by Grant No. W-31-109-ENG-38 from the Division of Materials Science, Office of Basic Energy Sciences at the U.S. Department of Energy, and at Portland State University by the National Science Foundation (Che-9632815) and the donors of the Petroleum Research Fund, administered by the American Chemical Society (ACS-PRF No 31099-AC1). This work has benefited from useful conversations with M.-H. Whangbo.

CM990240H